Characterization of Rapid Charging Events due to Sheath Capacitance and Impact on the International Space Station Plasma Hazard Process

William A. Hartman*[1], William. D. Schmidl[1], Ronald Mikatarian[1]
(1) The Boeing Company, Houston, USA

Abstract

During an Extravehicular Activity (EVA), if the Extravehicular Mobility Unit (EMU) makes galvanic contact with the International Space Station (ISS), a negative Floating Potential (FP) can lead to an arcing hazard when it exceeds -45.5 V, and a positive FP can produce a DC current high enough to stimulate the astronaut's muscles (5 mA), and also cause a hazard. The Boeing Space Environments team developed and utilizes a Plasma Interaction Model (PIM) in order to calculate the ISS FP based on the plasma environment, ISS velocity, geomagnetic field, solar array and ISS orientation, and solar array regulation to support EVA planning operations. Presently, the model excludes the sheath capacitance, resulting in the total potential drop being across the dielectric surface of the vehicle. Data from the Floating Potential Measurement Unit (FPMU) show this assumption to be generally true. However, Rapid Charging Events (RCE) are often observed in the FPMU data at eclipse exit when the electron number density, N_e, is low ($<$5e10 m^{-3}). During these events, the FP can rise more than 40 V in one to five seconds. There is then a relaxation phase where the FP drops back to the normal FP values. The PIM model is not capable of producing these RCEs. It was thought that the inclusion of the sheath in PIM could improve the charging predictions, particularly as related to RCEs. A parametric study was performed to determine what portion of the measured FP is across the sheath for a range of N_e experienced by the ISS, and if the inclusion of the sheath in PIM is necessary. Results show that the potential drop across the sheath is negligible at times when the $N_e > $ 1e11 m^{-3}. However, there appears to be a transitional region between 1e10 m^{-3} and 1e11 m^{-3} where the sheath capacitance becomes more significant. During those conditions the potential drop across the sheath can be larger than the potential drop across the dielectric for short periods (1-5 seconds). These results agree remarkably well with measurements made by the FPMU. The inclusion of the sheath explains why high charging measurements occur when the N_e is low at eclipse exit and even times when the solar arrays are not a significant driver (i.e., potentials often rise as the ISS flies through spread-F). Results also show that the RCEs are not a safety concern because the potential drop across the dielectric surface does not exceed -45.5 V. In that case, the EMU would not arc. This gives high confidence in the low probability of an arcing hazard occurring.

Background:

During an Extravehicular Activity (EVA), if the Extravehicular Mobility Unit (EMU) makes galvanic contact with the International Space Station (ISS), a negative Floating Potential (FP) can lead to an arcing hazard when it exceeds -45.5 V, and a positive FP can produce a DC current high enough to stimulate the astronaut's muscles (5 mA), and also cause a hazard. Due to these possible hazards, the capability to predict when such events may occur is necessary for EVA planning purposes.

The ISS plasma hazard process is based on the number of floating potential and current exceedances. The current exceedances are computed based on the ISS FP, and an assumed exposed current collecting area. The plasma hazard also includes the probability of contact between conductive surfaces on the suit and the ISS that were computed by the ISS Probability Risk Assessment (PRA) team based on ISS video observations of past EVAs. (private communication with NASA)

The Boeing Space Environments team developed and utilizes a Plasma Interaction Model (PIM) in order to calculate the ISS FP based on the plasma environment, ISS velocity, geomagnetic field, solar array and ISS orientation, and solar array regulation. The PIM is a time dependent model based on the divergence of current producing an accumulation of charge on the vehicle resulting from primary current sources: 1) Mast Wires (MW), 2) Solar Arrays (SA), and 3) Russian Segment (RS). Periodic current sources include the Plasma Contactor Units (PCU), and berthed or docked visiting vehicles such as the Japanese H-II Transfer Vehicle (HTV). Figure 1 is an illustration of the PIM circuit.
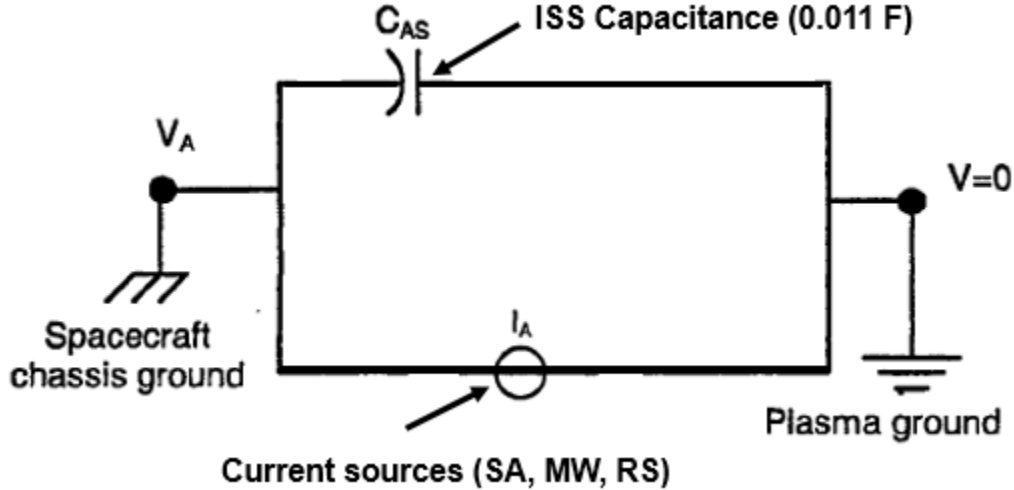
Figure 1: Illustration of PIM circuit

In this circuit, I_A represents the total current collected from the current sources (equation 1). Here SA represents the current collected form the solar arrays. Due to the charge accumulated on the coverglass restricting the current to the gaps where the electrons are collected between the solar cells, this current is modeled and cannot be represented by a simple equation. The second term is the sum of the ion currents collected by the multiple surfaces. In this case, E_0 is the ion ram energy, J_{ion} is the ion current density, and V_A is the potential of the surface collecting the ions. The third term is the electron currents. Again, the V_A represents the potential of the surface collecting the electrons J_{th} is the electron thermal current, and T_e is the electron temperature. The second and third terms assume that surfaces collect current as cylinders.

$$I_A = SA - \sum J_{ion} A \sqrt{1 - \frac{V_A}{E_0}} + \sum J_{th} A \sqrt{1 + \frac{V_A}{T_e}}$$ (eq 1)

Once I_A is calculated, it is applied to the ISS capacitance (0.11 F) for six seconds to determine the new ISS FP (equation 2).

$$V = \frac{1}{C_{ISS}} \int_0^t I_{ISS} dt + V_0$$ (eq 2)

Presently, the model excludes the sheath capacitance, resulting in the total potential drop being across the dielectric surface of the vehicle. Therefore, the charging rate in the PIM is completely controlled by the large ISS capacitance (11 mF) and the total current collected from the environment. This approach was presumed to be conservative because any potential drop across the sheath will not contribute to the dielectric breakdown during an arc.

Data from the Floating Potential Measurement Unit (FPMU) show this assumption to be generally true. The FPMU has been collecting electron number density (N_e), electron temperature (T_e), and FP data since 2006. During cases where the N_e is above $5e10$ m^{-3}, PIM does reasonably well with the removal of the sheath. Figure 2 is a plot showing the comparison of PIM predictions and FPMU measurements for eclipse exits when the $N_e > 5e10$ m^{-3}.
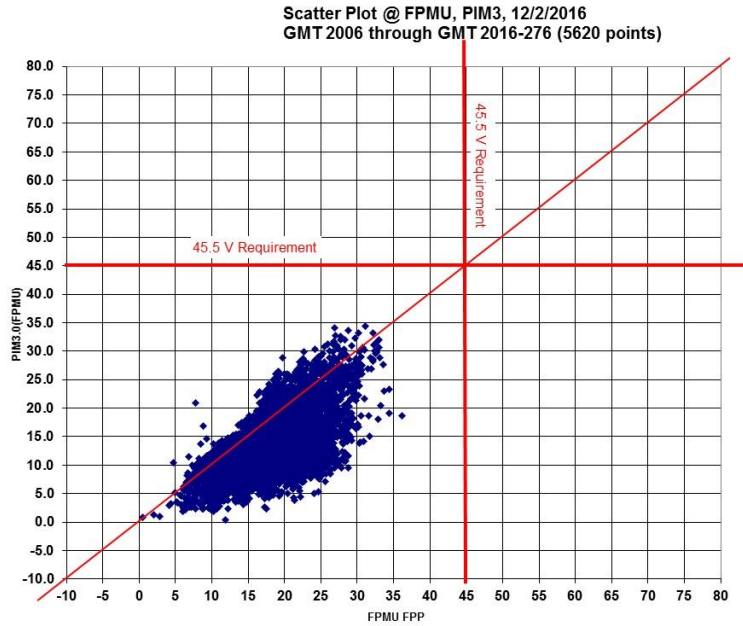
Figure 2: 45 degree plot comparing FPMU measurements and PIM calculations at eclipse exit for $N_e > 5e10$ m^{-3}.

However, in cases when the N_e is $< 5e10$ m^{-3}, the FP reaches potentials that can be much larger than the PIM predicts. Figure 3 is in the same format as figure 2, but includes eclipse exits with $N_e < 5e10$ m^{-3}. It is evident that the PIM does not capture the physics when the N_e is low.
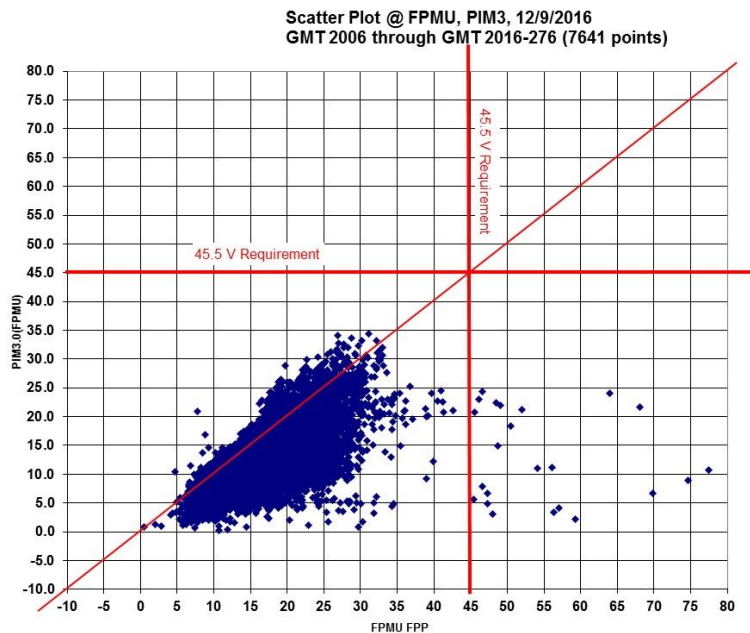

Figure 3: 45 degree plot comparing FPMU measurements and PIM calculations at eclipse exit for all N_e.

Normal and Rapid Charging Events

During normal conditions where the $N_e > 5e10$ m^{-3}, the ISS FP changes gradually, often taking 30 to 60 seconds to reach the maximum FP after eclipse exit. Figure 4 shows a normal eclipse exit charging event that occurred ~20.6 UT March 10, 2008. At this time, the N_e was 5e10 m^{-3}. The FP went from -21.5 to -33 V in 31 seconds. As shown in Figure 2, the PIM does well at producing these events
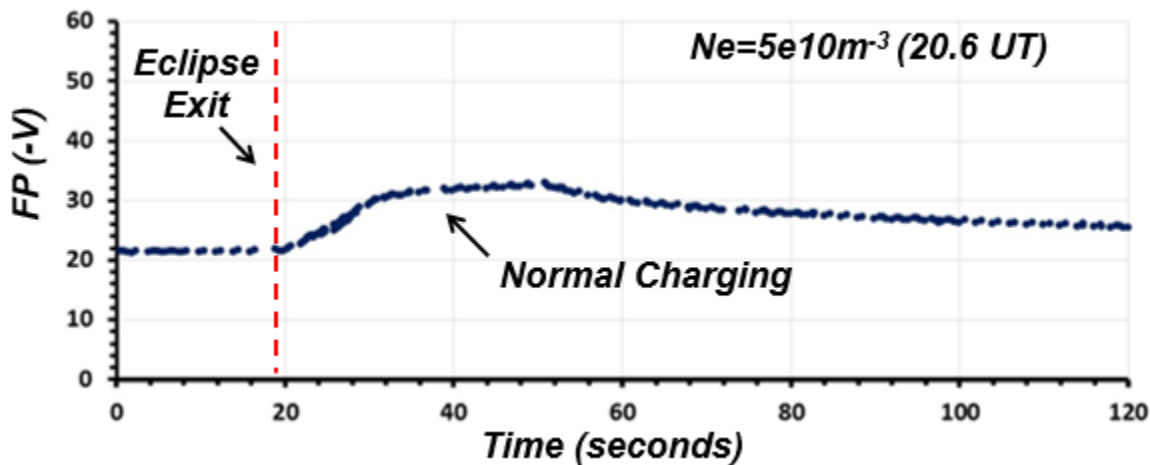
Figure 4: Plot of a normal eclipse exit that occurred 20.6 UT March 10, 2008

However, Rapid Charging Events (RCE) are often observed at eclipse exit when the N_e is low (<5e10 m^{-3}). During these events, the FP can rise more than 40 V in one to five seconds. There is, then, a relaxation phase where the FP drops back to the normal FP values. Figure 5 shows a RCE that occurred 8.4 UT on the same day as the normal charging event shown in Figure 4 (March 10, 2008). Being from the same day, most variables that affect ISS charging were consistent between the two events: ISS attitude, solar array orientation, eclipse exit latitude, and geomagnetic activity. The one significant difference between these two events was that the N_e at 8.4 UT was 1e10 m^{-3}. During the RCE, the FP went from -19.2 to -48.3 V in 1.2 seconds. The FP, then, relaxed to -20.5 V in 20 seconds and returned to what is considered normal ISS charging. In order to charge and discharge the ISS capacitance at that rate requires more current than the low N_e environment can provide. Presently, the PIM model is not capable of producing these RCEs.
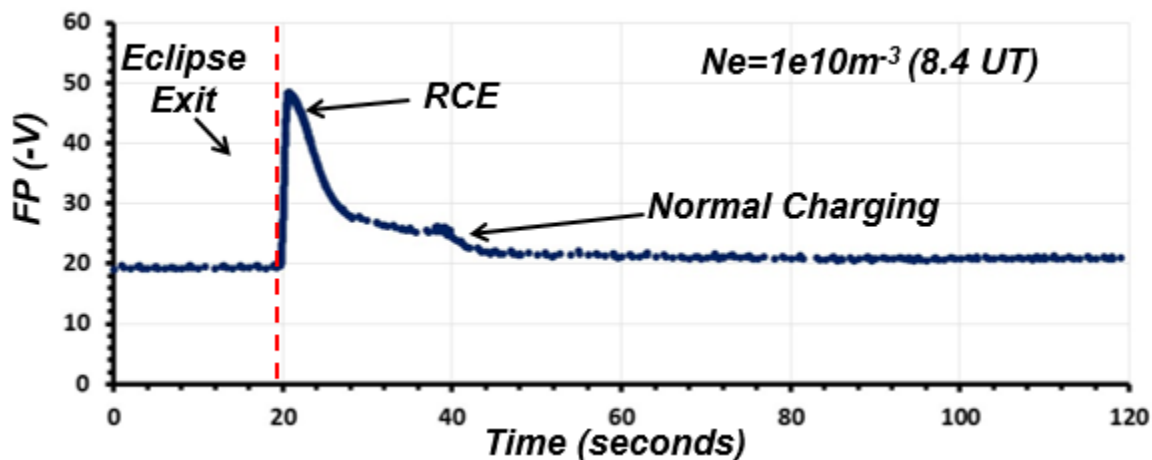

Figure 5: Plot of a RCE that occurred 8.4 UT March 10, 2008

Investigation
The inclusion of the sheath in series with the current collecting surfaces and the dielectric surfaces may be necessary to capture the physics during RCEs. In actuality, the sheath can support a noteworthy potential when the N_e is low. Figure 6 illustrates how the sheath would be included into the PIM circuit if the update was found to be necessary. The current contributions presently excluded from the PIM are surrounded by the red boxes. In this illustration, I_S is the direct current through the sheath surrounding the anodized aluminum, C_S is the capacitance of the sheath surrounding the anodized layer, and C_A is the capacitance of the sheath surrounding the exposed conducting areas.
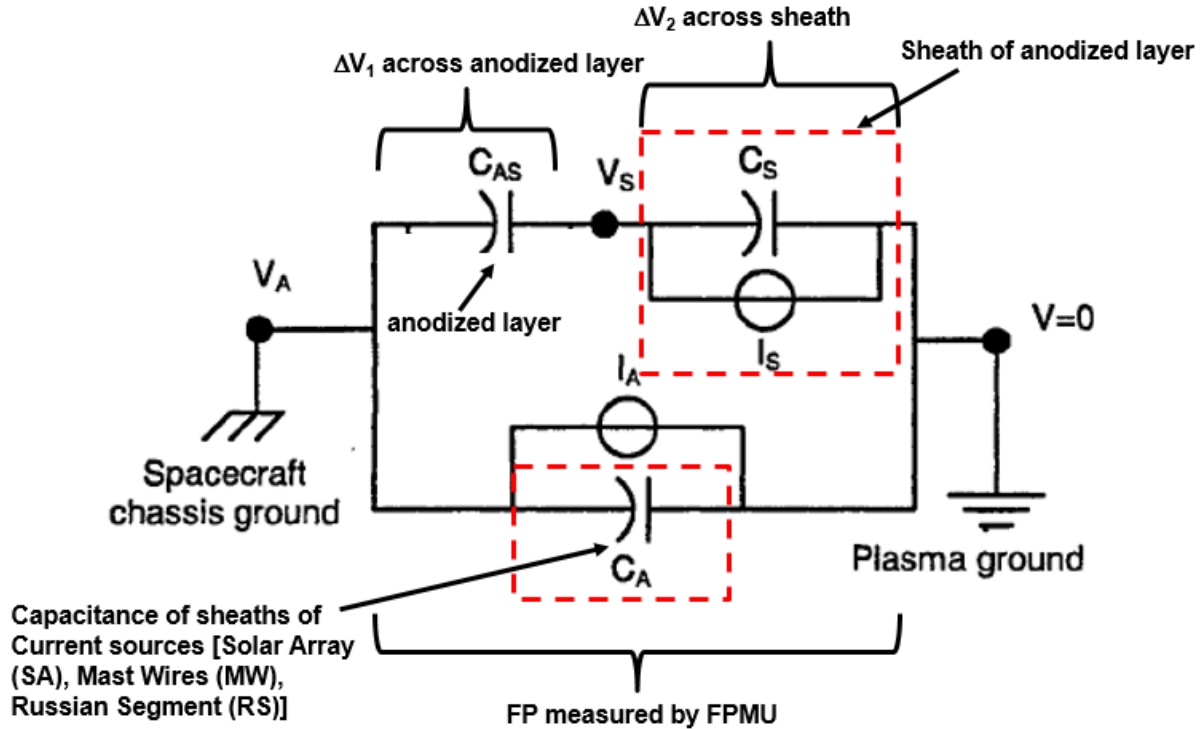
Figure 6: Illustration of how the sheath would be included into the PIM (figure adapted from "Spacecraft Charging Calculations NASCAP-2k and SEE Spacecraft Charging Handbook)

The sheath acts as a resistor and capacitor in parallel. Recall that the electron and ion current are dependent on J_{th} and J_{ion}, respectively.

$$J_{th} = qN_e\sqrt{\frac{qT_e}{2\pi m_e}}$$
(eq 3)

$$J_{ion} = qN_i v_{normal}$$
(eq 4)

As can be seen in equations 3 and 4, the current densities are functions of the N_e. During normal N_e conditions the sheath can support a current large enough that a significant potential cannot form across it. Therefore, in those cases neglecting the potential across the sheath is reasonable. However, if the N_e drops, then the plasma effectively becomes a resistor. If the resistance should become high enough during low N_e conditions, the contribution of the displacement current produced by the expansion of the sheath could result in a large potential across that region. Therefore, the small sheath capacitance could become significant. If the resistance in the sheath should drop due to a return back to normal N_e values, the charge in the sheath would then effectively drain from the capacitor through the low resistance in parallel and the potential would relax to a lower value. This could explain the relaxation phase observed many times in the FPMU data and shown in Figure 5.

A parametric study was performed to determine what portion of the measured FP is across the sheath for a range of N_e experienced by the ISS, and if the inclusion of the sheath in the PIM is necessary. The sheath capacitance above the anodized aluminum was estimated to be ~0.5 mF based on the size of the ISS. It is recognized that the sheath capacitance depends on the N_e, T_e and FP (*Chen*, 2006), but the sheath capacitances were treated as constants for this investigation.

Also, although the current from the solar arrays depends on the FP, the SA currents were initially treated as constant. In actuality, the current collected by the solar arrays is highly dependent on the ISS FP and decreases as the ISS charges to more negative FP. A test was performed in 2003 in order to determine what current the ISS was capable of collecting by correlating the electron current expelled from the Plasma Contactor Unit (PCU) to the FP measured

by the FPMU (Internal memo 2003_004 by John Kern). The PCU is capable of expelling 10 A of electron current. Results show that the PCU could control the ISS FP by emitting a current on the 1-100 mA range. Therefore, the total electron current collected on the ISS structure must be in that range. The currents collected on the SAs in the PIM are normally in the 5-50 mA range.

RCEs occur in about one to five seconds. In order to simplify this model, the SA current was set at 50 mA or 5 mA for one second and then cut off, allowing the FP to relax. The SA current and the N_e are not independent, but they are treated that way for this investigation. This should give a reasonable estimation to the maximum charging levels caused by a decaying current beginning at 50 or 5 mA and dropping to 0 in ~5 seconds.

In order to simplify this investigation, the current collected on the Mast Wires was neglected and the electric field caused by the ISS motion through the geomagnetic field was assumed to be 0 V/m. The SA and RS were the only current sources from the original PIM (reference). New additions to the circuit shown in Figure 7 included the displacement currents in the sheaths above anodized and conducting surfaces, along with the direct current in the sheath above the anodized aluminum.
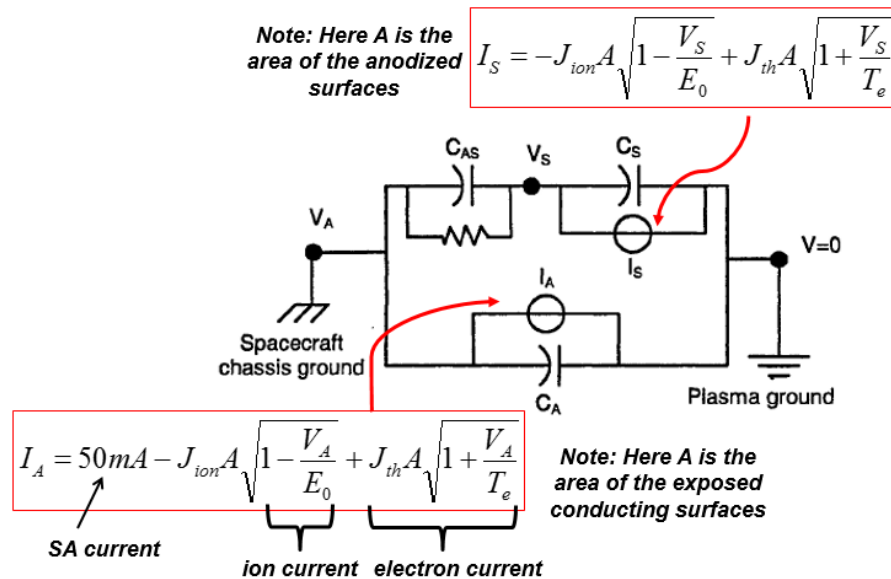
Note: Here A is the area of the anodized surfaces

$$I_S = -J_{ion}A\sqrt{1 - \frac{V_S}{E_0}} + J_{th}A\sqrt{1 + \frac{V_S}{T_e}}$$

C_{AS} V_S C_S

V_A $V=0$

I_A I_S

Spacecraft chassis ground

C_A Plasma ground

$$I_A = 50mA - J_{ion}A\sqrt{1 - \frac{V_A}{E_0}} + J_{th}A\sqrt{1 + \frac{V_A}{T_e}}$$

Note: Here A is the area of the exposed conducting surfaces

SA current

ion current   **electron current**

Figure 7: Illustration of how the equations were included (figure adapted from "Spacecraft Charging Calculations NASCAP-2k and SEE Spacecraft Charging Handbook)

A series of calculations was done with this setup to encompass a range of conditions experienced by the ISS. Unlike PIM applying constant currents for six seconds, these calculations were done in 0.001 second time steps. Figure 8 shows the potentials across the anodized aluminum and the sheath above the anodized layer when the N_e is 1e11 m^{-3}, the initial FP is 0 V, and the SA collect 50 mA for one second. At that N_e, the sheath is too conductive to support a significant potential. Most of the potential drop is across the anodized layer (-4.6 V). After the initial charging occurring for one second, the FP gradually returns to 0 V.
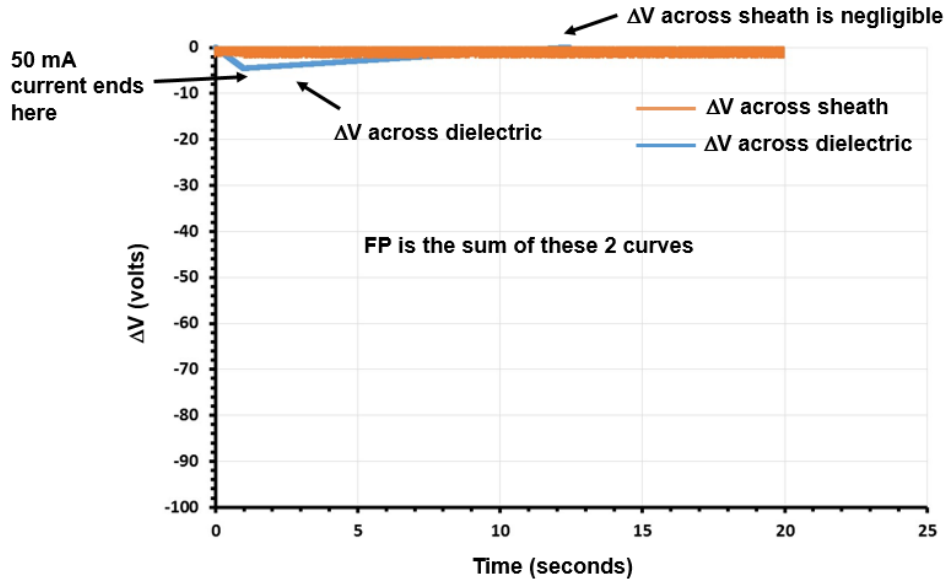
Figure 8: Plot of the ΔV across the anodized aluminum (blue) and the sheath (orange) when solar array current is 50 mA for 1 second and the N_e is 1e11 m^{-3}.

The next case was run with the following conditions: 1) the N_e is 1e10 m^{-3}, 2) the initial FP is 0 V, and 3) the SA collect 50 mA for one second. Unlike the first case where the N_e was 1e11 m^{-3}, there is a significant potential across the sheath while the ISS charges (Figure 9). The potential across the sheath reached -40.3 V. Interestingly, the potential across the anodized aluminum only reached -4.9 V. Once the SA current was turned off, the potential across the sheath dropped to ~0 V in about one second. The time for the potential across the anodized aluminum to relax was extended due to the smaller current that the exposed metallic area on the RS could collect from the lower N_e plasma.
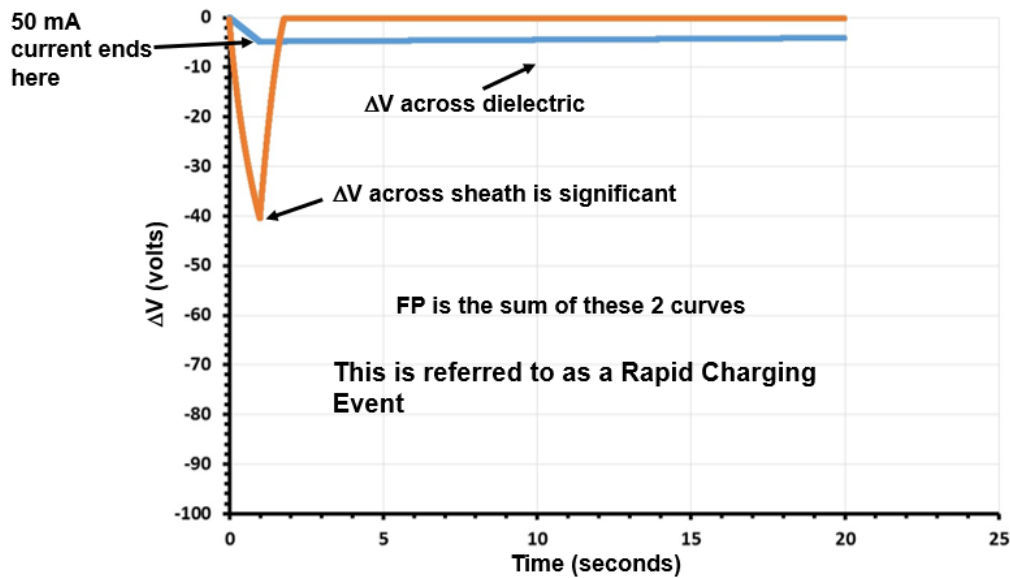

Figure 9: Plot of the ΔV across the anodized aluminum (blue) and the sheath (orange) when solar array current is 50 mA for 1 second and the N_e is 1e10 m^{-3}.

The last case for an initial FP of 0 V and an SA current of 50 mA was then run for N_e = 1e9 m^{-3} (Figure 10). The potential across the sheath reached -92 V. The potential across the dielectric was again -4.9 V, similar to the 1e10

m^{-3} case. The relaxation of the sheath took 13 seconds. The discharging of the potential across the anodized aluminum due to the ion current from the low N$_e$ environment is barely visible in the 20 seconds in Figure 10.
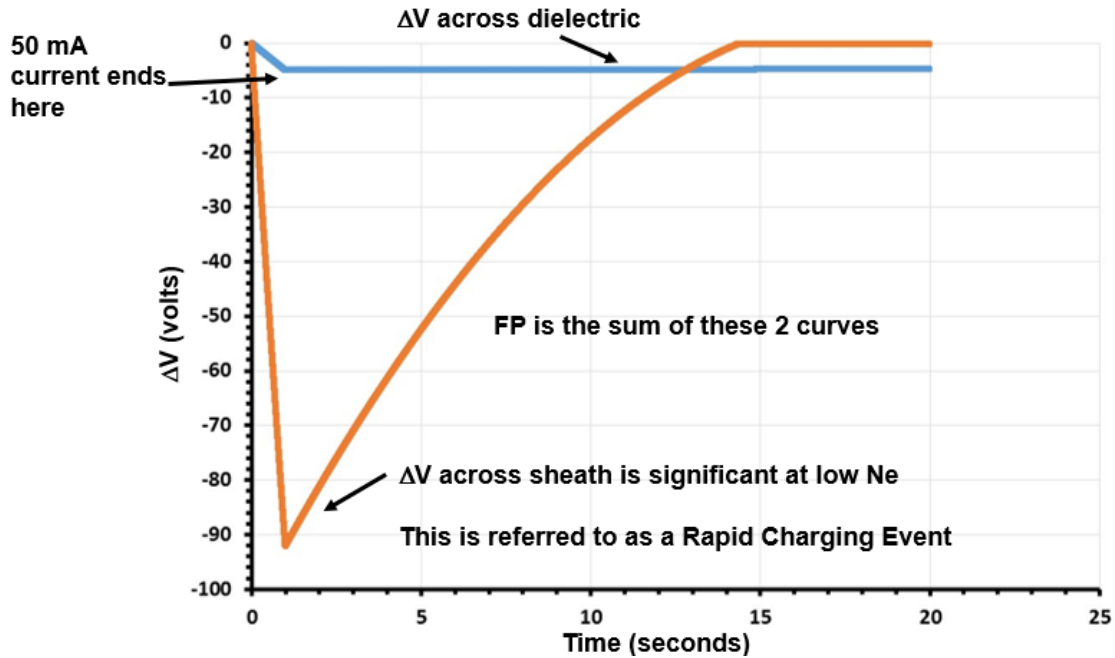

Figure 10: Plot of the ΔV across the anodized aluminum (blue) and the sheath (orange) when solar array current is 50 mA for 1 second and the N$_e$ is 1e9 m^{-3}.

Similar cases were run for different combinations of initial FP's, SA currents, and N$_e$ values. All cases show that the potential across the sheath becomes dominant at low N$_e$, although its amplitude becomes smaller as the SA current drops.

Case study
In order to check the sheath dependency with on-orbit data, cases were run using the measured N$_e$, T$_e$, and initial FP. A decaying SA current due to the changing FP was required. In reality, the SA current is highly dependent on the FP, but the FP was not used to calculate the SA current in this example. For simplification the SA current in the model was set to decay from 50 mA to 0 mA in three seconds. The model results were then compared to on-orbit FPMU data. One of the cases run was the RCE shown earlier in Figure 5. The results of the model and the measured FP are shown in Figure 11. Although not perfect, the model shows accurate maximum FP (~50 V) and resulting FP (~26 V) after the relaxation phase of the RCE. The model relaxation phase occurred more quickly than in the FP data. This is thought to be caused by the SA current never completely dropping to 0 like it is assumed in the model. A continuous, but lower, SA current would extend the relaxation time.
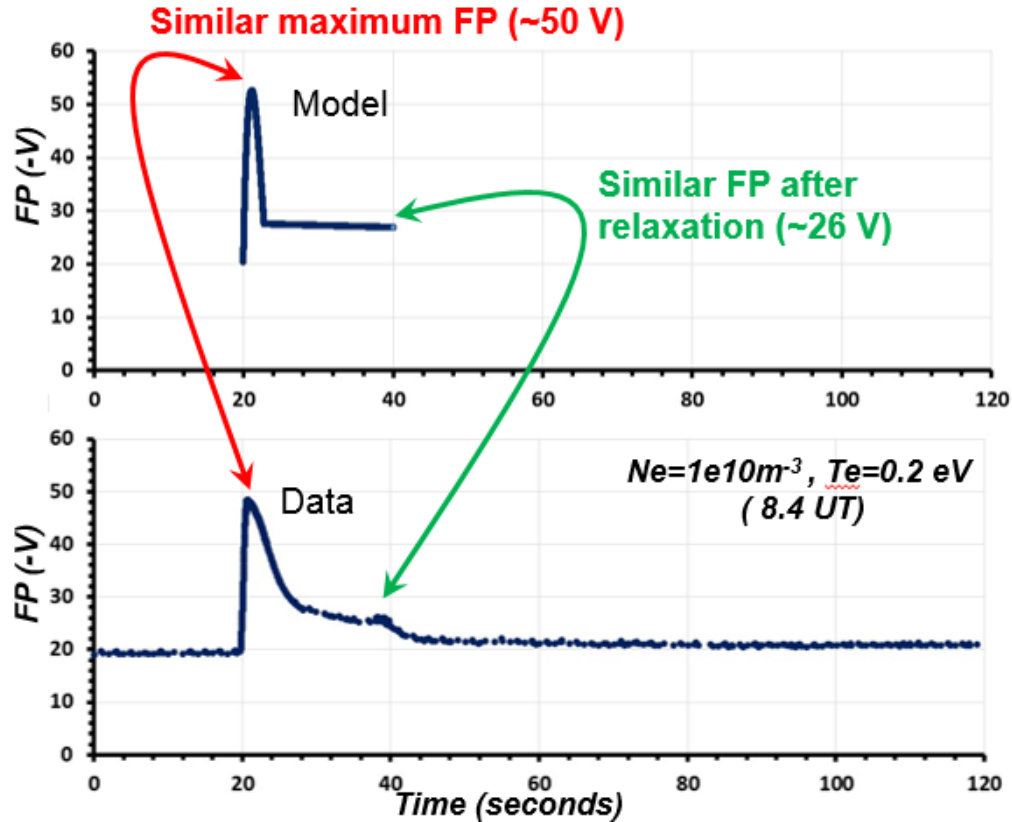
Figure 11: Comparing the FP from model and FPMU data from 8.4 UT March 10, 2008.

Charging During Spread-F

An unintended finding also came from this study. Small rises in the FP are often seen as the ISS flies through plasma depletions in eclipse. The FP, then, relaxes back to normal levels as the ISS exits the depletion and the N_e returns to normal values. An example is shown in Figure 12 where the ISS flew through a spread-F event. There is a small increase in the FP slope from 9.25 to 9.3 UT. At this same time the N_e had dropped from around 1e11 m^{-3} to about 1.4e10 m^{-3}. At 9.3 UT, the N_e returned to 1e11 m^{-3} and the FP dropped by ~1 V. Because the SAs are not illuminated, they would not contribute to the ISS charging at this time. However, based on the N_e dependence of the sheath capacitance found during this study, the potential across the sheath would be higher while the ISS was in the depletion region. No increase in the current collected on the ISS is needed to explain this event.
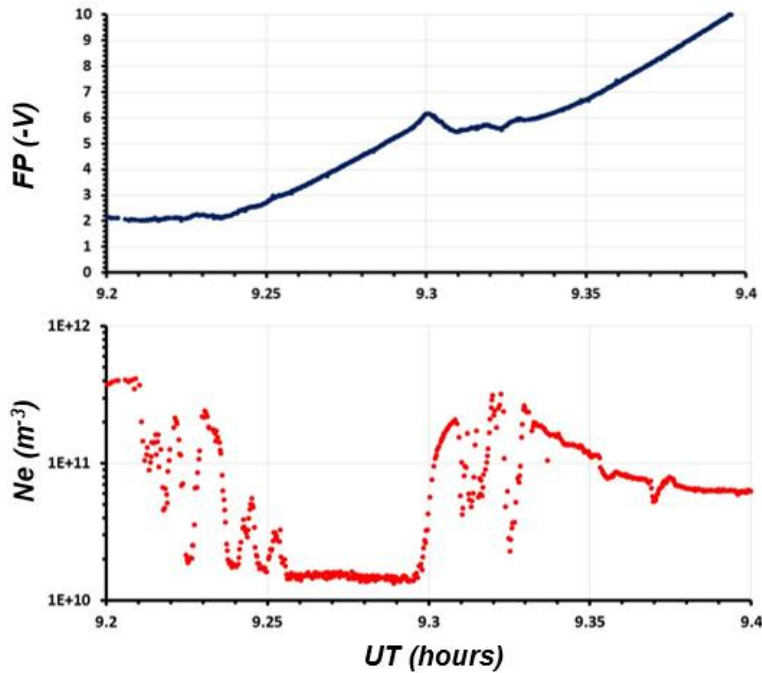
Figure 12: FP and N_e during a Spread-F event on March 9, 2008.

Conclusion

This study shows that the sheath can become the dominant driver of the ISS FP when the N_e is low (<1e11 m^{-3}). During those conditions the RCEs do not produce a significant potential across the anodized aluminum. This is an important result because the -45.5 V limit for arcing was determined by applying a range of potentials to aluminum 6061 coupons of different thicknesses in a high N_e plasma (Kramer and Hartman, 2015 EID684-16248). Based on this study, almost all of the potential was across the anodized layer in those test cases. Even in those conditions the time to arc was greater than 10 seconds. Because RCEs occur in less than 10 seconds, they were already considered to not be an arcing concern but still accounted for in the PRA. The Boeing Space Environments Team believes that this new study eliminates the RCEs as an arcing concern during EVAs because the potential across the anodized layer does not reach -45.5 V. The inclusion of the sheath also explains small charging events often seen as the ISS flies through spread-F. Including the sheath model would improve PIM results.

References
Chen, F. F. (2006), Time-varying impedance of the sheath on a probe in an RF plasma, Plasma Sources Sci. Technol, 15, doi:10.1088/0963-0252/15/4/022

Internal memo 2003_004 by John Kern
.
Kramer and Hartman, 2015 EID684-16248